Research Article

ENERGY EXPLORATION & EXPLOITATION

Energy Exploration & Exploitation
2019, Vol. 37(1) 355–374

DOI: 10.1177/0144598718800727
journals.sagepub.com/home/eea
SAGE

Enhanced oil recovery efficiency of low-salinity water flooding in oil reservoirs including Fe^{2+} ions

Yeonkyeong Lee, Hyemin Park, Jeonghwan Lee and Wonmo Sung

Abstract

The low-salinity waterflooding is an attractive eco-friendly producing method, recently, for carbonate reservoirs. When ferrous ion is present in the formation water, that is, acidic water, the injection of low-salinity water generally with neutral pH can yield precipitation or dissolution of Fe-minerals by pH mixing effect. $FeSO_4$ and pyrite can be precipitated and re-dissolved, or vice versa, while siderite and $Fe(OH)_2$ are insoluble which are precipitated, causing permeability reduction. Particularly, pyrite chemically reacts with low-salinity water and release sulfate ion, altering the wettability, favorably, to water-wet. In this aspect, we analyzed oil production focusing on dissolution of Fe-minerals and Fe-precipitation using a commercial compositional reservoir simulator. From the simulation results, the quantities of precipitation and dissolution were enormously large regardless of the type of Fe-minerals and there was almost no difference in terms of total volume in this system. However, among Fe-minerals, $Fe(OH)_2$ precipitation and pyrite dissolution were noticeably large compared to troilite, $FeSO_4$, and siderite. Therefore, it is essential to analyze precipitation or dissolution for each Fe-mineral, individually. Meanwhile, in dissolving process of pyrite, sulfate ions were released differently depending on the content of pyrite. Here, the magnitude of the generated sulfate ion was limited at certain level of pyrite content. Thus, it is necessary to pay attention for determining the concentration of sulfate ion in designing the composition of injection water. Ultimately, in the investigation of the efficiency of oil production, it was found that the oil production was enhanced due to an additional sulfate ion generated from FeS_2 dissolution.

Department of Earth Resources and Environmental Engineering, Hanyang University, Seoul, Republic of Korea

Corresponding authors:
Wonmo Sung, Department of Earth Resources and Environmental Engineering, Hanyang University, 222 Wangsimni-ro, Seongdong-gu, Seoul 04763, Republic of Korea.
Email: wmsung@hanyang.ac.kr
Jeonghwan Lee, Department of Energy & Resources Engineering, College of Engineering, Chonnam National University, 77 Yongbong-ro, Buk-gu, Gwangju 61186, Korea.
Email: jhwan@jnu.ac.kr

Keywords
Low-salinity, ferrous ion, permeability, wettability, oil production, carbonate

Introduction

Low-salinity waterflooding (LSWF) is a simple and environmentally friendly enhanced oil recovery (EOR) method, which can improve the oil recovery by lowering the salinity of injected brine or by adjusting the ion concentration. The recovery of oil from carbonates is below 30% since more than 80% of carbonate reservoirs possess intermediate or oil wetness (Mahmoud and Nasr-El-Din, 2014; Yue and Wang, 2015; Zhou and Yang, 2017). Through various experimental studies, it has been verified that the injection of low-salinity water (LSW) to an oil-wet carbonate reservoir has been able to alter its wettability to water-wet (Morrow et al., 1998; Standnes and Austad, 2000; Yassin et al., 2015). Besides, the salinity of injection water and the concentration of potential determining ions (PDI) such as sulfate ion (SO_4^{2-}), Ca^{2+}, and Mg^{2+} have been reported to be major factors leading to a wettability alteration (Al-Shalabi et al., 2014; Jalilian et al., 2017; Salamat et al., 2016; Yousef et al., 2011; Zhang et al., 2007). Lager et al. (2007), McGuire et al. (2005), and Wolthers et al. (2008) confirmed that LSW injection caused the dissolution of calcite and an increase in pH due to OH^- ions generated from the dissolution as follows

$$H_2O + CaCO_3 \leftrightarrow Ca^{2+} + HCO_3^- + OH^- \quad (1)$$

In other words, an increase in pH by 1 to 3 was observed as calcite within the core became dissolved through the LSWF experiments. Since there was only one equilibrium point among the oil, brine, and rock, at a specific pH, the change in pH shifted the chemical equilibrium, which could result in precipitation (Mahani et al., 2015). Zhang and Sarma (2012) demonstrated the precipitation of $CaSO_4$ in pores, increasing the pressure difference during the LSW injection.

When ferrous ion (Fe^{2+}) ion is contained in formation water or injection water, Fe^{2+} ion as well as Ca^{2+} and Mg^{2+} can also affect the alteration in wettability. Haugen (2016) experimentally confirmed that Fe^{2+} in brines had been oxidized to Fe^{3+}, and it had a greater influence on wettability than Ca^{2+} cation. Also, Fjelde et al. (2017) performed a laboratory experiment to investigate the effect of Fe^{2+} oxidation and cation bridging by Fe^{3+} on wettability, and they observed that low concentration of Fe^{3+} increased the oil wetness of rock surface and altered the wettability to less water-wet. Also, Fe^{2+} ion can react with anions such as SO_4^{2-}, HCO_3^-, and OH^-, yielding precipitates of $FeSO_4$, siderite ($FeCO_3$), and Fe $(OH)_2$, respectively. Al-Saiari et al. (2008) measured the quantity of $FeCO_3$ precipitation when the Fe^{2+} to Ca^{2+} molar ratio in the FW was varied and identified that 60% of the Fe^{2+} precipitated. Particularly among the Fe-precipitations, the low solubility of $FeCO_3$ and $Fe(OH)_2$ could directly affect the permeability reduction (Stumm and Lee, 1961).

Fe-minerals are present deep underground; for instance, pyrite (FeS_2), which is one of the most common sulfides in sedimentary rocks, can often be found in carbonates that are rich in organic materials (Clavier et al., 1976). When Fe-minerals such as FeS_2, troilite (FeS), and $FeCO_3$ exist in carbonates, the increase in pH changes during LSW injection can generally

lead to the dissolution of Fe-minerals (Hanor, 1994; Liu and Millero, 2002; Rickard and Luther, 2007).

In the case of the acidic reservoir with a low pH condition, FeS_2 can be easily dissolved as mentioned in the following research works. Nicol et al. (2013) performed a laboratory experiment on the dissolution of FeS_2 and confirmed that FeS_2 dissolved to a greater extent in a solution with a low concentration of SO_4^{2-} such as formation water. Wolfe et al. (2016) observed through a FeS_2 dissolution experiment that FeS_2 dissolved into iron and sulfur within a solution at pH 3; iron predominantly existed in the form of Fe^{2+} ions and sulfur existed as SO_4^{2-} ions. According to these experimental results, the permeability change could have been caused by the dissolution of FeS_2 when it was present in carbonates. As well, EOR effects could be observed due to the generation of SO_4^{2-} ions via the FeS_2 dissolution.

Previous studies have focused on the optimum ion composition leading to the maximum oil recovery from a carbonate reservoir by modifying the concentrations of SO_4^{2-}, Ca^{2+}, and Mg^{2+} in LSW. It has been suggested that increasing the concentration of SO_4^{2-} rather than Ca^{2+} and Mg^{2+} was more effective toward improving the recovery of oil (Fathi et al., 2010; Shariatpanahi et al., 2011; Sohal et al., 2016; Strand et al., 2006; Zhang et al., 2006). However, there has not yet been an analytical study with regard to EOR effects in consideration of precipitation and dissolution due to geochemical reactions when LSWF was applied to the carbonate reservoir containing a large quantity of Fe^{2+} ions in the FW and Fe-minerals in carbonates. Additionally, Fe-minerals have different solubilities depending on the type of mineral; some are insoluble, and thus, the permeability change could have occurred due to the reactions with LSW.

In this study, we analyzed the dissolution and precipitation of Fe-minerals resulting from geochemical reactions during the injection of LSW in the presence of Fe-minerals in carbonates. Also, Fe-mineral dissolution generated SO_4^{2-} and these ions promoted Fe-precipitation. Since this could lead to a change in permeability, in addition to EOR effects of the LSW injection, there may have been additional effects on improving the oil recovery. Therefore, we intended to explain the relationships between reservoir temperature, SO_4^{2-} concentration, and oil recovery by analyzing the change in dissolution and precipitation of Fe-minerals depending on the temperature and Fe-mineral content within carbonates.

Governing equation

Darcy's law governs the flow of fluids in porous media. Multiple components within the aqueous phase can also be attributed to the behavior of fluids, such as dispersion and diffusion. The general partial differential flow equation for the multi-component in the fluids and mineral species is as follows

$$\frac{\partial}{\partial x}\left(y_{il}\frac{\rho_o \beta_c A k_x k_{ro}}{\mu_o}\frac{\partial P}{\partial x}\right)\Delta x + q_l + V\sigma_{i,m} = \frac{V_b}{\alpha_c}\frac{\partial}{\partial t}(\varnothing \rho_l S_l y_{il}) \tag{2}$$

where $l =$ oil, gas, or water and $i = 1, 2, \ldots, n_c$. n_c represents the number of species in fluids and mineral. As LSW is injected into the formation, the composition of formation water is changed with time. In a commercial compositional reservoir simulator GEM of Computer Modeling Group Ltd, the change of the composition in formation water is then

calculated from the flow equations of aqueous phase representing of n_c components in aqueous phase.

The material balance equations for multi-component fluid flow have been provided in an adaptive-implicit manner by Collins et al. (1992) and Siu et al. (1989). Nghiem et al. (2011) have also introduced aqueous phase behavior and chemical reactions within compositional simulations. The material balance finite difference equation for the multiple components and species is as follows

$$\Delta T_l y_{il} \Delta P_l^{n+1} + V\sigma_{i,m}^{n+1} = \frac{V_{b_i}}{\alpha_c \Delta t}\left[(\varnothing \rho_l S_l y_{il})_i^{n+1} - (\varnothing \rho_l S_l y_{il})_i^{n}\right] - q_l \tag{3}$$

In this equation, q_l is the source/sink term and $V\sigma_{i,m}$ is the reaction term for rate-dependent reactions. Symbols α_c and β_c are the unit conversion factors, and other symbols are described in Appendix.

The reaction term ($V\sigma_{i,m}$) of i, m in equations corresponds to the rate of precipitation and dissolution as follows

$$V\sigma_{i,m}^{n+1} = VS_w \sum_{i=1}^{n_c} v_i r_i \tag{4}$$

where v_i are the stoichiometry coefficients of component i and in equation (4), r_i is the reaction rate per unit bulk volume of rock, which is calculated through the following equation

$$r_i = A_i k_i \left(1 - \frac{Q_i}{K_{eq,i}}\right) \tag{5}$$

$$Q_i = \prod_{i=1}^{n_c} a_i^v \tag{6}$$

If the reaction rate, r_i, is positive ($(Q_i/K_{eq,i}) < 1$), mineral precipitation occurs; if the rate is negative ($(Q_i/K_{eq,i}) > 1$), mineral dissolution occurs, where A_i is the reactive surface area and k_i is the rate constant. In this simulation, the initial values of A_i and k_i were set as 100 m^2/m^3 (A_{0i}) and 1.58×10^{-9} mol/m^2s (k_{0i}). These values were initially set as the same for six different minerals. As chemical reactions process into the equilibrium state, the values of A_i and k_i for different minerals were calculated by the equations shown in Table 1. In the case of k_i, since initial value of k_i (k_{0i}) is extremely small, the calculated values were almost same for different minerals as listed in Table 1. And also, Q_i is the activity product of mineral reaction i, $K_{eq,i}$ is the chemical equilibrium constant for mineral reaction i, and a_i denotes the activity of component i. A modified Debye–Hückel model is preferred to calculate the activity determined by the molality, temperature, and ionic strength (Mistry and Lienhard, 2013). The chemical equilibrium constant $K_{eq,i}$ represents the temperature-dependent constant, and tables of the $K_{eq,i}$ values are provided by Delany and Lundeen (1991) and Kharaka et al. (1988). In equation (5), chemical reaction is progressed until the chemical equilibrium, in which Q_i is equal to $K_{eq,i}$ (Ma et al., 2015). In this study, chemical

Table 1. The reactive surface are (A_i) and the rate constant (k_i) after two pore volumes injected at location Ⓐ.

	$Fe(OH)_2$	$FeCO_3$	$FeSO_4$	FeS	FeS_2	$CaCO_3$
A_i (m^2/m^3)	3.76×10^{13}	1.27×10^{2}	4.14×10^{5}	7.95×10	2.70×10	9.97×10
k_i (mol/m^2s)	9.39×10^{-8}	9.39×10^{-8}	9.39×10^{-8}	9.39×10^{-8}	9.39×10^{-8}	9.39×10^{-8}

reactions for calcite and Fe-minerals with low-salinity injection water containing SO_4^{2-} are applied and the involved chemical reaction equations are as follows

$$H^+ + CaCO_3 \leftrightarrow Ca^{2+} + HCO_3^- \tag{7}$$

$$CaSO_4 \leftrightarrow Ca^{2+} + SO_4^{2-} \tag{8}$$

$$2H^+ + Fe(OH)_2 \leftrightarrow Fe^{2+} + 2H_2O \tag{9}$$

$$FeSO_4 \leftrightarrow Fe^{2+} + SO_4^{2-} \tag{10}$$

$$H_2O \ + FeS_2 \leftrightarrow 0.25H^+ + 0.25SO_4^{2-} + Fe^{2+} + 1.75HS^- \tag{11}$$

$$H^+ + \mathrm{FeS} \leftrightarrow Fe^{2+} + HS^- \tag{12}$$

$$H^+ + FeCO_3 \leftrightarrow Fe^{2+} + HCO_3^- \tag{13}$$

In the above equations, reaction to the right direction denotes dissolution and precipitation for left direction.

Equations of Ai

$$A_i = A_{0i}\frac{N_i}{N_{0i}}$$

where

A_{0i} the reactive surface area at time zero,
N_i the mole of mineral per unit grid block bulk volume at current time, and
N_{0i} the mole of mineral per unit grid block bulk volume at time zero.

Equations of ki

$$k_i = k_{0i}\exp\left[-\frac{E_{ai}}{R}\left(\frac{1}{T}-\frac{1}{T_0}\right)\right]$$

where

k_{0i} the rate constant at time zero,
E_{ai} the activation energy,

Figure 1. One-dimensional carbonate reservoir system.

R the gas constant (8.314 J/mol K),
T the current temperature, and
T_0 reference temperature.

In this study, we used a commercial compositional reservoir simulator GEM of Computer Modeling Group Ltd. for compositional and chemical modelling. In this simulator for describing LSWF, the geochemical reacting mechanisms are selectively considered. Meanwhile, all mechanisms are involved simultaneously in the case of experiment. In this aspect, the simulational work is limited comparing to experimental work in describing the geochemical reactions. The flow equations are discretized using the adaptive-implicit method. The adaptive implicit selects a block's implicitness dynamically during the computation and is useful complex reservoir. The Jacobian matrix is solved by Incomplete LU factorization followed by the generalized minimal residual method iterative method.

Reservoir model

The numerical one-dimensional simulation model was created with 51 grid blocks of the same width and thickness having a length of 1400 ft. As shown in Figure 1, injection well and production well were set to be at both ends of model. The model was carbonate rock composed of 90% calcite. Its pore volume was 605,895 ft^3, the initial oil saturation was 88%, and the original oil in place was 70,114 bbl. The porosity and absolute permeability were 0.27 and 30 md. The initial pressure and temperature were set to 3810 psia and 120°C under isothermal conditions. Since the relative permeability is the most critical factor on oil recovery, which has the greatest uncertainty, we applied the relative permeability from the experiments of Yousef et al. (2011) to this study by performing the history matches with the SO_4^{2-} concentration (Beretta and Gyftopoulos, 2015; Yousef et al., 2011). Figure 2 illustrates the relative permeability curves during the initial and shifted states after wettability alteration by the LSW injection. These curves would be shifted depending on the concentration of SO_4^{2-} ions in aqueous, which play a major role in detaching oil and altering the wettability. In the production well, the operating pressure was specified at 1500 psia as boundary condition of right-end of the system. In the injection well, the injection rate of 70 bbl/day was specified as boundary condition at the left-end of the system. When the injection pressure was over the upper limit of 4000 psi, this pressure was set as boundary condition. The LSW was injected at the start of production and the injection rate was set to 1–2 ft/day so that the chemical reaction could occur sufficiently. The period of injection and production was 2 years for which two pore volumes were injected.

In this paper, in order to construct the simulation model for the application of LSWF to the carbonate reservoir containing Fe^{2+} ions in the FW and Fe-minerals within rock, 910 ppm of Fe^{2+} ions were included in the FW, and FeS_2, FeS, and $FeCO_3$ were present in the

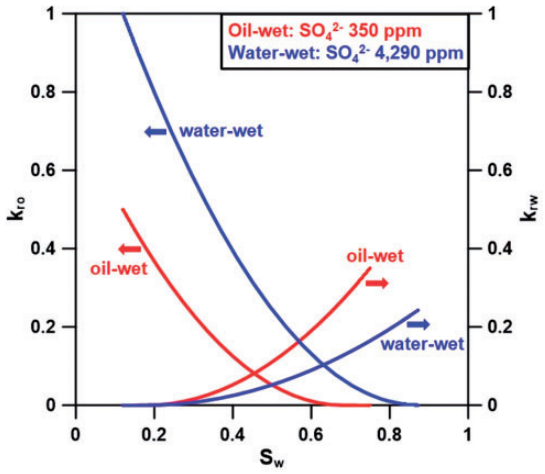

Figure 2. Relative permeability curves used in the simulation when the wettability changes from oil-wet to water-wet (Yousef et al., 2011).

carbonate rock at content of 1.0%, 1.0%, and 0.5%, respectively (Table 2). Table 3 summarizes the ionic compositions and concentrations of the FW and injection water. The data of the FW ware at initial state, which was in equilibrium with the rocks before the injection of LSW. They were based on the ionic compositions of the FW in the Middle East where Fe^{2+} ions were present amid a low pH of 3.2. The total dissolved solids of the FW were as high as 150,000 ppm; the Ca^{2+} concentration was especially high due to the dissolution of calcite ($CaCO_3$), which accounted for 90% of the carbonate rock. In the case of the injection water, the seawater composition used in the laboratory coreflooding experiment by Yousef et al. (2011) was taken. Although the salinity of the seawater was twice as high as that of typical ocean seawater, it was a third of the FW salinity, so it was suitable for LSW. The injection water was set to a pH 7.8, with reference to the pH of the Persian Gulf.

Results and discussion

pH change analysis

Within this study, a simulation was performed for the application of LSWF in the oil reservoir, where Fe-minerals exist in carbonate rock with Fe^{2+} ions in the FW as given in Table 2. When LSW was injected into the carbonate reservoir, Fe-mineral dissolution and precipitation occurred as the pH increased, which was the main factor influencing the chemical reactions. Thus, we examined the dissolution and precipitation as a factor of pH change. The initial pH of the FW containing 910 ppm of Fe^{2+} ions was 3.2, which was relatively low as shown in Figure 3; however, the pH at the location of Ⓐ near the injection well drastically increased to 4.0 as a result of the LSW injection. At the time of one pore volume injected (1 PVI), the mixing effects with the LSW (pH 7.8) prevailed at location Ⓐ, which promoted the dissolution of Fe-minerals (Chen et al., 2012). However, at the location Ⓑ far from the injection well, the pH for 1 PVI remained in the initial state due to the little effect by LSW

Table 2. Fe-mineral content in carbonate rock and the Fe^{2+} ion concentration in the formation water.

Fe-minerals contained in carbonate rock	FeS_2	1.0%
	FeS	1.0%
	$FeCO_3$	0.5%
Fe^{2+} ion concentration in formation water		910 ppm

Table 3. Input data for ion composition and concentrations (Yousef et al., 2011).

Ion	*Formation water (ppm)*	*Injection water (ppm)*
Na^+	17,009	18,300
Ca^{2+}	37,876	650
Mg^{2+}	425	2110
Fe^{2+}	910	0
Cl^-	95,291	32,200
SO_4^{2-}	260	4290
HCO_3^-	0	120
TDS	151,800	57,670

TDS: total dissolved solids.

injection. However, at the time of two pore volume injected (2 PVI), the pH was stabilized to 4.0 at the locations Ⓐ and Ⓑ since the mixing effects were stabilized by the injection of LSW for a long period of time. It could also be considered that the chemical reactions between ions were nearly equilibrated. Therefore, due to the above phenomena, we quantitatively analyzed the dissolution and precipitation of Fe-minerals at location Ⓐ after 2 PV injected with sufficient chemical reactions.

Precipitation and dissolution of minerals

As LSW was injected into the carbonate reservoir, the chemical equilibrium was broken due to differences in the ionic composition and concentration between the FW and injection water, resulting in the dissolution and precipitation of rock. Figure 4 shows the total dissolution and precipitation quantities of Fe-minerals regardless of type at location Ⓐ. The quantity of Fe-precipitation was 264.4×10^3 gmol and the quantity of Fe-mineral dissolution was 264.8×10^3 gmol at 2 PVI; there was almost no difference in terms of the total volume in this system. The difference was very small, but the quantity of dissolution or precipitation itself was as large as 264×10^3 gmol. Thus, it was necessary to analyze the quantity of precipitation and dissolution in detail for each Fe-mineral. This was because the quantity of precipitation and dissolution caused by chemical reactions between the ionic composition of the FW, the injection water, and the mineral constituents of the carbonate rock were different for each type of Fe-minerals. Also, since the solubility or insolubility characteristics of each Fe-mineral were different, the permeability changed accordingly. The precipitation and dissolution quantities for each Fe-mineral were estimated as can be seen in Figure 5. In this figure, a positive value for the change in mineral moles indicated precipitation, while a negative value denoted dissolution. At the time of 2 PVI, a noticeable increase in the quantity of $Fe(OH)_2$ precipitation and FeS_2 dissolution yielded

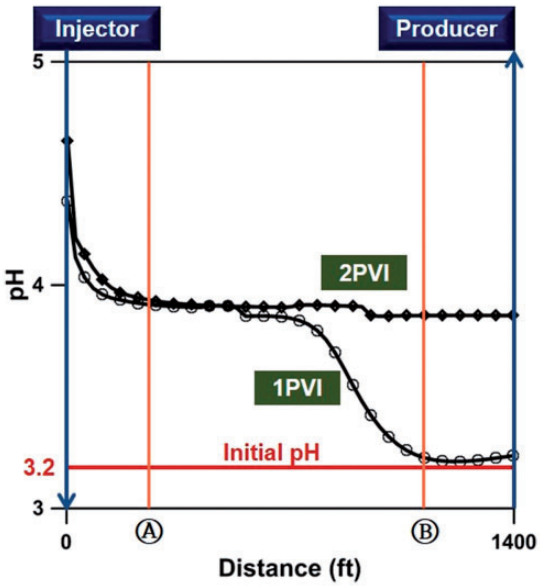

Figure 3. Distribution of pH values after low-salinity water injection.

220×10^3 gmol and 200×10^3 gmol, respectively. These quantities were significantly higher compared to the quantities for the other Fe-minerals, such as $FeCO_3$, $FeSO_4$, FeS, and the carbonate, $CaCO_3$. In the case of $Fe(OH)_2$, it was not contained within carbonate rock but was generated via precipitation; while FeS_2 existing within the carbonates was dissolved. The aspect for $Fe(OH)_2$ and FeS_2 precipitation or dissolution relative to each injection time is depicted in Figure 6. The reason for the significantly larger quantities of precipitation and dissolution for these two minerals compared to the other minerals could be comprehended from the equilibrium constants for the chemical reactions. The equilibrium constants could be defined as a function of temperature as follows

$$\log K_{eq} = a_0 + a_1 T + a_2 T^2 + a_3 T^3 + a_4 T^4 \tag{14}$$

where K_{eq} is the equilibrium constant, a_i is the chemical equilibrium coefficient, and T is the reservoir temperature. In this study, the equilibrium constant values and activity product values are summarized in Tables 4 to 6 according to the chemical equilibrium coefficients for each mineral reaction at a reservoir temperature of 120°C (Bethke, 1996). As shown in the results, $Fe(OH)_2$ precipitated because the saturation index (Q/K_{eq}), which was a ratio of the activity product to the equilibrium constant, was 6.26E-6 smaller than 1, while the (Q/K_{eq}) of FeS_2 was 5.03E + 8 and much larger than 1, resulting in the dissolution of FeS_2.

The reaction for the precipitation of $Fe(OH)_2$, possessing an enormously large equilibrium constant, can be seen in equation (9) as being independent of the SO_4^{2-} ions. On the other hand, FeS_2 dissolved when contacting the injection water, resulting in the generation of 0.25 mol of SO_4^{2-} ions (equation (11)). The FeS_2 dissolution is also attributed to the generation of hydrogen sulfide (H_2S) which can cause the problems for souring of oil

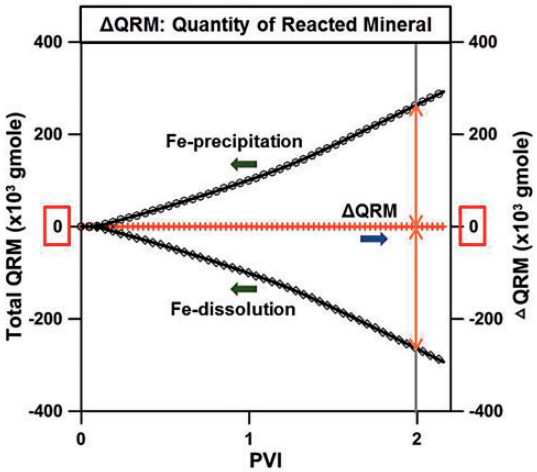

Figure 4. The quantity of reacted minerals for the Fe-precipitation and Fe-dissolution at location Ⓐ.

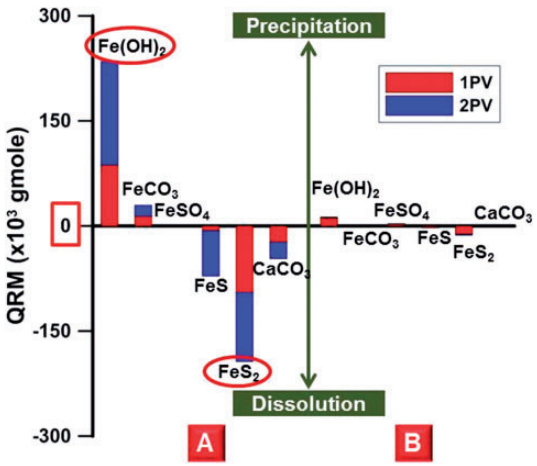

Figure 5. The quantity of precipitation and dissolution for Fe-minerals and calcite at locations Ⓐ and Ⓑ.

(Al-Kindi et al., 2008). However, in this simulation study, the amount of H_2S was not enough to occur the souring problem during the period of production. Also, we focused on the effect of mineral precipitation and dissolution on the recovery of oil. In wettability alteration mechanism, SO_4^{2-} ions played a major role in enhancing the oil recovery by detaching oil that had attached on the carbonate rock surface forming an oil-wet condition and by causing the alteration in wettability. The initial SO_4^{2-} concentration of the FW in this study was 260 ppm and that of LSW was 4290 ppm. As LSW was injected into the carbonate reservoir where FeS_2 did not exist, the SO_4^{2-} concentration increased to about 2300 ppm due to simple mixing effects without the additional generation of SO_4^{2-} ions (Figure 7).

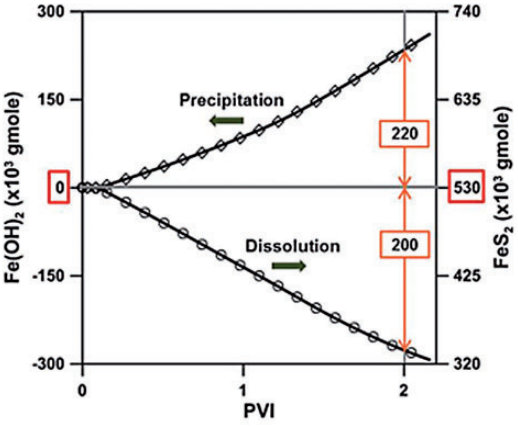

Figure 6. The quantity of reacted minerals for $Fe(OH)_2$ and FeS_2 at location Ⓐ.

Table 4. Chemical equilibrium coefficients (a_i) used for calculation of the equilibrium constants (K_{eq}) (Bethke, 1996).

	a_0	a_1	a_2	a_3	a_4
$Fe(OH)_2$	1.43×10	-6.18×10^{-2}	2.02×10^{-4}	-3.78×10^{-7}	2.19×10^{-10}
$FeCO_3$	2.54×10^{-1}	-1.94×10^{-2}	9.48×10^{-6}	1.17×10^{-7}	-4.12×10^{-10}
$FeSO_4$	3.71	-4.32×10^{-2}	7.96×10^{-6}	2.49×10^{-7}	-7.60×10^{-10}
FeS	−3.67	-2.87×10^{-3}	-5.38×10^{-5}	2.42×10^{-7}	-5.19×10^{-10}
FeS_2	-2.65×10	8.16×10^{-2}	-4.05×10^{-4}	1.15×10^{-6}	-1.66×10^{-9}
$CaCO_3$	2.07	-1.43×10^{-2}	-6.06×10^{-6}	1.46×10^{-7}	-4.19×10^{-10}

However, in the presence of FeS_2 in carbonate rock, SO_4^{2-} ions were released from the dissolution of FeS_2 as LSW was injected and the additional SO_4^{2-} ion concentration reached up to 960 ppm, which played a notably important role with regard to improving the efficiency of the LSWF method. Therefore, to analyze these reactions in more detail, we examined the occurrence of SO_4^{2-} ions depending on the temperature and content of FeS_2, which were the primary factors influencing the above reactions.

In order to investigate the effect of the reservoir temperature and FeS_2 content on the generation of SO_4^{2-} from the FeS_2 dissolution, we first performed a simulation using K_{eq} in Table 5 for reservoir temperatures from 50 to 120°C in intervals of 10°C. After 2 PV was injected, the quantity of dissolved FeS_2 increased by 6.4 times when the temperature was 120°C compared to 50°C, which indicated that higher reservoir temperatures yielded more SO_4^{2-} ions due to the dissolution of FeS_2, thereby improving the EOR efficiency through LSWF. Then, simulations for the effects of FeS_2 content were performed when FeS_2 was contained within carbonate rock from 0 to 8.5%, over 0.5% intervals. Figure 8 shows the additional SO_4^{2-} ions from the FeS_2 dissolution at the time of 2 PV injected, except for simple mixing effects due to the injection of LSW. As a result, the SO_4^{2-} concentration was

Table 5. Chemical equilibrium constants (K_{eq}) for various temperatures.

	Equilibrium constant (K_{eq})							
	50°C	*60°C*	*70°C*	*80°C*	*90°C*	*100°C*	*110°C*	*120°C*
$Fe(OH)_2$	4.45E+11	1.66E+11	6.60E+10	2.78E+10	1.24E+10	5.83E+09	2.87E+09	1.47E+09
$FeCO_3$	2.10E–01	1.40E–01	9.45E–02	6.44E–02	4.43E–02	3.08E–02	2.16E–02	1.53E–02
$FeSO_4$	3.95E+01	1.55E+01	6.19E+00	2.52E+00	1.04E+00	4.39E–01	1.88E–01	8.19E–02
FeS	1.21E–04	1.03E–04	8.71E–05	7.28E–05	6.05E–05	4.99E–05	4.10E–05	3.35E–05
FeS_2	4.78E–24	1.39E–23	3.64E–23	8.63E–23	1.87E–22	3.75E–22	6.99E–22	1.22E–21
$CaCO_3$	2.27E+01	1.65E+01	1.20E+01	8.84E+00	6.53E+00	4.85E+00	3.62E+00	2.72E+00

Table 6. Activity product at 120°C after two pore volumes injected.

	$Fe(OH)_2$	*$FeCO_3$*	*$FeSO_4$*	*FeS*	*FeS_2*	*$CaCO_3$*
Activity product (Q)	9.20×10^{3}	3.58×10^{-5}	1.24×10^{-7}	1.88×10^{-4}	6.14×10^{-13}	1.98×10^{-3}
Saturation index (Q/K_{eq})	6.26×10^{-6}	2.34×10^{-3}	1.51×10^{-6}	5.61	5.03×10^{8}	7.28×10^{-4}

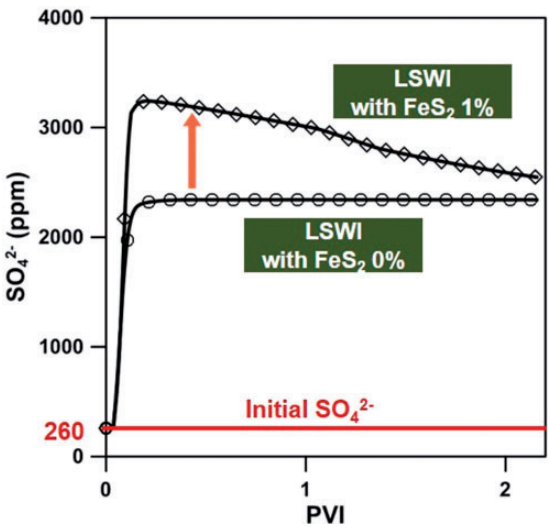

Figure 7. The occurrence of SO_4^{2-} ions due to the FeS_2 dissolution at location Ⓐ.

close to the maximum when 7% or more FeS_2 existed within the carbonate reservoir of 120 C. Meanwhile, the quantity of generated SO_4^{2-} at 50 C was less than that at 120 C and SO_4^{2-} ions did not occur any longer even when the content of FeS_2 was 1% or more. Therefore, since the EOR effect due to SO_4^{2-} ions was limited at certain temperatures and FeS_2 content levels, it is necessary to pay attention to the determination of the SO_4^{2-} concentration for the design of PDI compositions in LSW.

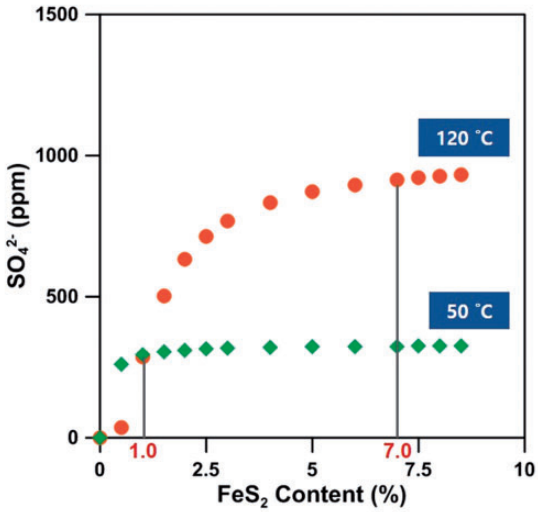

Figure 8. The additional SO_4^{2-} ions due to the FeS_2 dissolution depending on the FeS_2 content at location Ⓐ.

Permeability change and EOR effect analysis

When LSW was injected into the carbonate reservoir containing Fe-minerals, the precipitation or dissolution that occurred due to chemical reactions caused a permeability change (Figure 9). The simulation results analyzing this phenomenon showed that the pore volumes decreased by 250 ft^3 and increased by 270 ft^3 due to precipitation and dissolution including calcite dissolution, respectively, after 2 PV injections at location Ⓐ. Among the volumes, the volume reduction due to Fe-precipitation was 250 ft^3 and the volume increase due to the dissolution of Fe-minerals was 210 ft^3, with the exceptions of the precipitation and dissolution of calcite ($CaCO_3$). This indicated that the Fe-minerals precipitated more easily as opposed to dissolution. The pore volume change due to the dissolution and precipitation of Fe^{2+} is 40 ft^3, which is 6.6×10^{-5} times the model total pore volume 605,895 ft^3. This is almost negligible with respect to the total pore volume. Accordingly, the porosity was estimated as 27.09%, in which the change of porosity is also negligible; permeability was calculated using the Kozeny–Carman equation as follows

$$\frac{k}{k^0} = \left(\frac{\varnothing}{\varnothing^0}\right)^3 \left(\frac{1-\varnothing^0}{1-\varnothing}\right)^2 \tag{15}$$

This equation is one of the most widely accepted and simplest model for the permeability–porosity relationship, which provides a link between media properties and flow resistance in pore channels (Carman, 1937; Kozeny, 1927). The estimated permeability depending on the temperature and FeS_2 content is summarized in Table 7. As shown in the results, both quantities of precipitation and dissolution were very large; however, there was little difference between the two. Thus, it was confirmed that the permeability did not

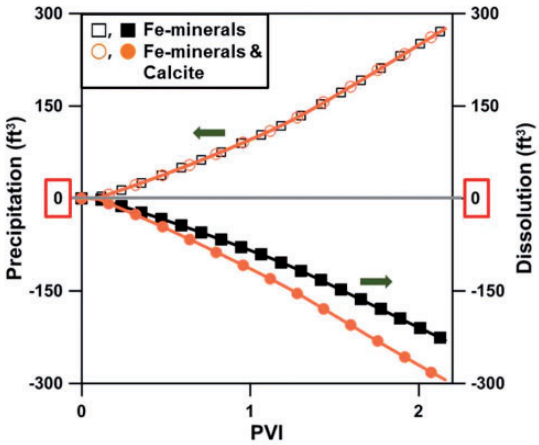

Figure 9. The estimated volumes of precipitation and dissolution at location Ⓐ.

Table 7. Permeability change at location Ⓐ due to precipitation and dissolution after two pore volumes injected.

T/FeS_2	*Precipitation (gmol)*	*Dissolution (gmol)*	*Initial permeability (md)*	*Changed permeability (md)*
50°C/1%	4.23×10^4	4.97×10^4	30	30.06
120°C/1%	2.64×10^5	3.11×10^5	30	30.39
120°C/8.5%	1.97×10^5	2.45×10^5	30	30.83

change from the initial value of 30 md. Also, the permeability did not change even when the reservoir temperature was lowered to 50°C or the FeS_2 content was increased to a value as high as 8.5%.

Finally, we investigated the EOR effect when LSWF was applied to the carbonate reservoir. In our system, there was almost no difference between the quantities of Fe-precipitation and Fe-mineral dissolution, it seems that the concentration of Fe^{2+} ion was almost not changed in this system, which would not affect the wettability of rock surface. Additionally, since Fe^{2+} was contained only in the formation water as 910 ppm, not in injection water, the concentration of Fe^{2+} was reduced up to 11 ppm by injecting the LSW of 0 ppm. In this aspect, we assumed that the effect of Fe^{2+} on wettability alteration was considered to be negligible. Therefore, in this paper, we mainly focused on the effect of precipitation and dissolution of Fe-minerals on oil recovery. In the case of carbonate rock containing FeS_2 as a Fe-mineral, as FeS_2 was dissolved, SO_4^{2-} ions were generated. These ions detached oil from the rock surface, and consequently, more oil was produced. As the results shown in Figure 10, the oil recovery for carbonates without FeS_2 was 69.06%, which was 12.41% greater than 56.65% for conventional WF due to the injection of LSW containing SO_4^{2-} ions. However, 76.67 and 76.70% were recovered from carbonates containing 1 and 8.5% FeS_2. This was much higher than that for conventional WF. Figure 11 shows schematically overall process in the absence and presence of FeS_2. In the case of its absence,

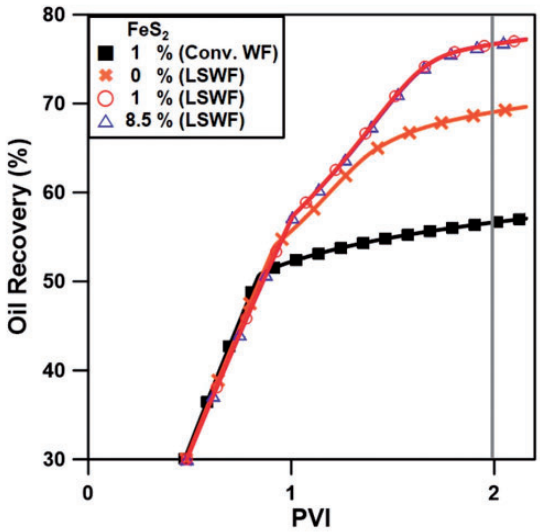

Figure 10. A comparison of the oil recovery depending on the FeS_2 content.

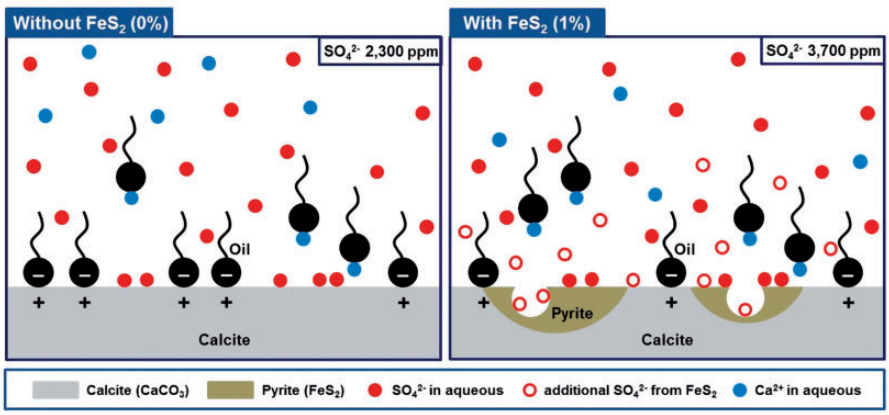

Figure 11. Schematic representation for oil detachment due to additional SO_4^{2-} ions from FeS_2.

some SO_4^{2-} ions in injection water attach on the carbonate rock surface, then oil is detached from rock surface. On the other hand, when FeS_2 is contained in carbonate rock, FeS_2 is dissolved releasing SO_4^{2-} ions near the rock surface. Therefore, more SO_4^{2-} ions can attach on rock surface causing the detachment of more oil. However, additional oil was not recovered for FeS_2 contents above 1%. This was because the total aqueous SO_4^{2-} concentration equilibrated to 3700 ppm after 2 PV injected when the FeS_2 content was 1% or more; thus, additional oil was not produced by the SO_4^{2-} ions. Since the equilibrium SO_4^{2-} ion concentration was 2300 ppm in the absence of FeS_2, this difference in the SO_4^{2-} concentration led to an additional 7.61% recovery of oil.

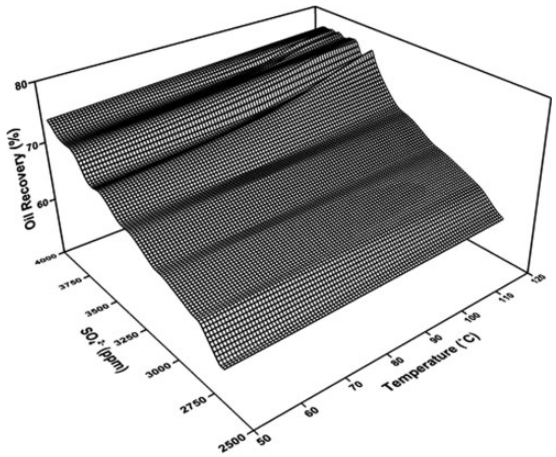

Figure 12. The oil recovery in relation to temperature and SO_4^{2-}.

Based on the above results, when applying LSWF to the carbonate reservoir containing Fe-minerals, we proposed an oil recovery relationship as a function of the temperature and SO_4^{2-} concentration in order to determine the optimal SO_4^{2-} concentration with regard to designing the PDI composition in LSW. A correlation between the oil recovery and SO_4^{2-} ion concentration, which was the most important PDI in LSW, and the reservoir temperature, which greatly affected the precipitation and dissolution of Fe-minerals, is represented in Figure 12.

Summary and conclusions

In this study, we performed several simulations to analyze the EOR effects focusing on the dissolution of Fe-minerals and Fe-precipitation when LSW containing SO_4^{2-} was injected into carbonate oil reservoirs.

From the results investigating precipitation and dissolution of Fe-minerals, it was found that the magnitude of precipitation and dissolution due to chemical reactions during LSW injections was enormously large, and the quantities were quite different according to the type of Fe-minerals. Among the Fe-minerals, the amounts of $Fe(OH)_2$ precipitation and FeS_2 dissolution were noticeably large in this system compared to FeS, $FeSO_4$, and $FeCO_3$, i.e. $Fe(OH)_2$ not contained in carbonate rock was precipitated, which is insoluble. On the other hand, FeS_2 contained in the rock was dissolved. This could be attributed by the saturation index criteria which was calculated by the ratio of activity product to equilibrium constant in the chemical reactions. As mentioned above, since the solubility characteristics of each Fe-mineral are different, it is essential to analyze precipitation or dissolution for each Fe-mineral individually, in which these phenomena yielded a permeability change (increase or decrease). However, in the case of this system, there was almost no difference between precipitation and dissolution in terms of total quantities of Fe-mineral, and consequently permeability was not changed.

From the analysis results for the SO_4^{2-} ions released from the process of precipitation and dissolution, in the dissolving process of FeS_2, the additional SO_4^{2-} ions were released

differently depending on the content of FeS_2. However, because the generation of SO_4^{2-} ion was limited at certain level of FeS_2 content in carbonate rock, it is necessary to pay attention to the determination of SO_4^{2-} concentration for the design of PDI compositions in the injection water. Ultimately, in the investigation of EOR efficiency, oil production was enhanced due to additional SO_4^{2-} ions generated from the FeS_2 dissolution.

Declaration of conflicting interests

The author(s) declared no potential conflicts of interest with respect to the research, authorship, and/or publication of this article.

Funding

The author(s) disclosed receipt of the following financial support for the research, authorship, and/or publication of this article: This work was supported by a grant funded as part of the project "Development of IOR/EOR technologies and field verification for carbonate reservoir in UAE" by the Korean Government Ministry of Trade, Industry and Energy (MOTIE) (No. 20152510101980).

ORCID iD

Wonmo Sung http://orcid.org/0000-0001-5795-4524

References

Al-Kindi A, Prince-Wright R, Walsh J, et al. (2008) Challenges for waterflooding in a deepwater environment. *SPE Production & Operations* 23(3): 404–410.

Al-Saiari HA, Yean S, Tomson MB, et al. (2008) Iron (II)-calcium carbonate: precipitation interaction. In: *SPE international oilfield scale conference, Aberdeen*, UK, 28–29 May 2008, SPE Paper 114064.

Al-Shalabi EW, Sepehrnoori K and Delshad M (2014) Mechanisms behind low salinity water injection in carbonate reservoirs. *Fuel* 121: 11–19.

Beretta GP and Gyftopoulos EP (2015) What is a chemical equilibrium state? *Journal of Energy Resources Technology* 137(2): 4.

Bethke (1996) *Geochemical Reaction Modeling: Concepts and Applications*. New York: Oxford University Press.

Carman PC (1937) Fluid flow through granular beds. *Institution of Chemical Engineering* 15: 150–166.

Chen J, Qui X, Fang Z, et al. (2012) Removal mechanism of antibiotic metronidazole from aquatic solutions by using nanoscale zero-valent iron particles. *Chemical Engineering Journal* 181–182: 113–119.

Clavier C, Heim A and Scala C (1976) Effect of pyrite on resistivity and other logging measurements. In: *SPWLA 17th annual logging symposium*, Denver, Colorado, 9–12 June 1976.

Collins DA, Nghiem LX, Li Y-K, et al. (1992) An efficient approach to adaptive-implicit compositional simulation with an equation of state. *SPE Reservoir Engineering* 7(2): 259–264.

Delany JM and Lundeen SR (1991) *The LLNL thermochemical data base – revised data and file format for the EQ3/6 package. Technical Report. Contract NO. W-7405-ENG-48, Lawrence Livermore National Laboratory*, California, USA.

Fathi SJ, Austad T and Strand S (2010) Smart water as a wettability modifier in chalk: the effect of salinity and ionic composition. *Energy & Fuels* 24(4): 2514–2519. https://doi.org/10.1021/ef901304m.

Fjelde I, Omekeh AV and Haugen PE (2017) Effect of ferrous ion Fe2+ on wettability. In: *79th EAGE conference and exhibition*, Paris, France, 12–15 June 2017.

Hanor JS (1994) Origin of saline fluids in sedimentary basins. *Geological Society of London Special Publications* 78(1): 151–174.

Haugen PE (2016) *Characterization of wettability alteration by flotation*. Master's Thesis, University of Stavanger, Norway.

Jalilian M, Pourafshary P, Sola BS, et al. (2017) Optimization of smart water chemical composition for carbonate rocks through comparison of active cations performance. *Journal of Energy Resources Technology* 139(6): 9.

Kharaka YK, Gunter WD, Aggarwal PK, et al. (1988) *SOLMINEQ. 88: a computer program for geochemical modeling of water-rock interactions. U.S. Geological Survey. Water-Resources Investigations Report 88–4227*. California: Menlo Park.

Kozeny J (1927) Uber kapillare leitung der wasser in boden. *Royal Academy of Science* 136: 271–306.

Lager A, Webb KJ and Black CJJ (2007) Impact of brine chemistry on oil recovery. In: *14th European symposium on improved oil recovery*, Cairo, Egypt, 22–24 April 2007.

Liu X and Millero FJ (2002) The solubility of iron in seawater. *Marine Chemistry* 77(1): 43–54.

Ma D, Liu C and Cheng C (2015) New relationship between resistivity index and relative permeability. *Journal of Energy Resources Technology* 137(3): 7.

McGuire PL, Chatham JR, Paskvan FK, et al. (2005) Low salinity oil recovery: an exciting new EOR opportunity for Alaska's north slope. In: *SPE western regional meeting*, Irvine, CA, 30 March–1 April 2005, SPE Paper 93903. https://doi.org/10.2118/93903-MS.

Mahani H, Keya AL, Berg S, et al. (2015) Insights into the mechanism of wettability alteration by low-salinity flooding (LSF) in carbonates. *Energy & Fuels* 29(3): 1352–1367.

Mahmoud M and Nasr-El-Din H (2014) Challenges during shallow and deep carbonate reservoirs stimulation. *Journal of Energy Resources Technology* 137(1): 8.

Mistry KH and Lienhard VJH (2013) Effect of nonideal solution behavior on desalination of a sodium chloride solution and comparison to seawater. *Journal of Energy Resources Technology* 135(4): 10.

Morrow NR, Tang G, Valat M, et al. (1998) Prospects of improved oil recovery related to wettability and brine composition. *Journal of Petroleum Science and Engineering* 20(3–4): 267–276.

Nghiem L, Shrivastava V and Kohse B (2011) Modeling aqueous phase behavior and chemical reactions in compositional simulation. In: *SPE reservoir simulation symposium*, Woodlands, Texas, 21–23 February 2011, SPE Paper 141417. https://doi.org/10.2118/141417-MS.

Nicol M, Miki H and Basson P (2013) The effects of sulphate ions and temperature on the leaching of pyrite. 2. Dissolution rates. *Hydrometallurgy* 133: 182–187.

Rickard D and Luther GW (2007) Chemistry of iron sulfides. *Chemical Reviews* 107(2): 514–562.

Salamat Y, Perez CAR and Hidrovo C (2016) Performance characterization of a capacitive deionization water desalination system with an intermediate solution and low salinity water. *Journal of Energy Resources Technology* 138(3): 5.

Shariatpanahi SF, Strand S and Austad T (2011) Initial wetting properties of carbonate oil reservoirs: effect of the temperature and presence of sulfate in formation water. *Energy & Fuels* 25(7): 3021–3028.

Siu A, Rozon B, Li Y-K, et al. (1989) A fully implicit thermal wellbore model for multi-component fluid flows. In: *SPE California regional meeting*, Bakersfield, California, 5–7 April 1989, SPE Paper 18777, https://doi.org/10.2118/18777-MS.

Sohal MA, Thyne G and Søgaard EG (2016) Review of recovery mechanisms of ionically modified waterflood in carbonate reservoirs. *Energy & Fuels* 30(3): 1904–1914.

Standnes DC and Austad T (2000) Wettability alteration in chalk. 2. Mechanism for wettability alteration from oil-wet to water-wet using surfactants. *Journal of Petroleum Science Engineering* 28(3): 123–143.

Strand S, Høgnesen EJ and Austad T (2006) Wettability alteration of carbonates – effects of potential determining ions (Ca^{2+} and SO_4^{2-}) and temperature. *Colloids and Surfaces A: Physicochemical and Engineering Aspects* 275(1–3): 1–10.

Stumm W and Lee GF (1961) Oxygenation of ferrous iron. *Industrial & Engineering Chemistry* 53: 143–146.
Wolfe AL, Stewart BW, Capo RC, et al. (2016) Iron isotope investigation of hydrothermal and sedimentary pyrite and their aqueous dissolution products. *Chemical Geology* 427: 73–82.
Wolthers M, Charlet L and Cappellen PV (2008) The surface chemistry of divalent metal carbonate minerals; a critical assessment of surface charge and potential data using the charge distribution multi-site ion complexation model. *American Journal of Science* 308: 905–941.
Yassin MR, Ayatollahi S, Rostami B, et al. (2015) Micro-emulsion phase behavior of a cationic surfactant at intermediate interfacial tension in sandstone and carbonate rocks. *Journal of Energy Resources Technology* 137(1): 12.
Yousef AA, Al-Saleh S, Al-Kaabi A, et al. (2011) Laboratory investigation of the impact of injection-water salinity and ionic content on oil recovery from carbonate reservoirs. *SPE Reservoir Evaluation & Engineering* 14(5): 578–593.
Yue W and Wang JY (2015) Feasibility of waterflooding for a carbonate oil field through whole-field simulation studies. *Journal of Energy Resources Technology* 137(6): 8.
Zhang P, Tweheyo MT and Austad T (2006) Wettability alteration and improved oil recovery in chalk: the effect of calcium in the presence of sulfate. *Energy & Fuels* 20(5): 2056–2062.
Zhang P, Tweheyo MT and Austad T (2007) Wettability alteration and improved oil recovery by spontaneous imbibition of seawater into chalk: impact of the potential determining ions Ca^{2+}, Mg^{2+}, and SO_4^{2}. *Colloids and Surfaces A: Physicochemical and Engineering Aspects* 301(1–5): 199–208.
Zhang Y and Sarma H (2012) Improving waterflood recovery efficiency in carbonate reservoirs through salinity variations and ionic exchanges: a promising low-cost "smart-waterflood" approach. In: *Abu Dhabi international petroleum exhibition and conference, Abu Dhabi, UAE*, 11–14 November 2012, SPE Paper 161631.
Zhou D and Yang D (2017) Scaling criteria for waterflooding and immiscible CO_2 flooding in heavy oil reservoirs. *Journal of Energy Resources Technology* 139(2): 13.

Appendix

Notation

A reactive surface area
n_c gaseous, aqueous, mineral components
N mole of mineral per unit grid block bulk volume
k permeability
P pressure
q injection/production rate
S saturation of phase l
t time
T transmissibility $T_l = \beta_c \frac{Ak_x}{\Delta x} \frac{k_{rl}\rho_l}{\mu_l}$

y_{ij} mole fraction of component i in phase l
α unit conversion coefficient
β unit conversion coefficient
ϕ porosity
μ viscosity
ρ_l molar density of phase l

Superscripts

n	old time level
$n+1$	new time level

Subscripts

g	gas
i	*component*
m	mineral
o	oil
w	water